Published in final edited form as:
Magn Reson Imaging. 2011 February ; 29(2): 185–193. doi:10.1016/j.mri.2010.08.006.

Development of T2-relaxation Values in Regional Brain Sites during Adolescence

Rajesh Kumar[1], **Sean Delshad**[1], **Paul M. Macey**[2,3], **Mary A. Woo**[2], and **Ronald M. Harper**[1,3,*]

[1]Department of Neurobiology, David Geffen School of Medicine at UCLA, University of California at Los Angeles, Los Angeles, CA 90095-1763, USA

[2]School of Nursing, University of California at Los Angeles, Los Angeles, CA 90095-1702, USA

[3]Brain Research Institute, University of California at Los Angeles, Los Angeles, CA 90095-1761, USA

Abstract

Brain tissue changes accompany multiple neurodegenerative and developmental conditions in adolescents. Complex processes that occur in the developing brain with disease can be evaluated accurately only against normal aging processes. Normal developmental changes in different brain areas alter tissue water content, which can be assessed by magnetic resonance (MR) T2-relaxometery. We acquired proton-density and T2-weighted images from 31 subjects (mean age ± SD, 17.4 ± 4.9 years; 18 male), using a 3.0-Tesla MR imaging scanner. Voxel-by-voxel T2-relaxation values were calculated, and whole-brain T2-relaxation maps constructed and normalized to a common space template. We created a set of regions-of-interest (ROIs) over cortical gray and white matter, basal ganglia, amygdala, thalamic, hypothalamic, pontine and cerebellar sites, with sizes of ROIs varying from 12 to 243 mm^3; regional T2-relaxation values were determined from these ROIs and normalized T2-relaxation maps. Correlations between R2 (1/T2) values in these sites and age were assessed with Pearson's correlation procedures, and gender differences in regional T2-relaxation values were evaluated with independent-samples t-tests. Several brain regions, but not all, showed principally positive correlations between R2 values and age; negative correlations emerged in the cerebellar peduncles. No significant differences in T2-relaxation values emerged between males and females for those areas, except for the mid pons and left occipital white matter; males showed higher T2-relaxation values over females. The findings indicate that T2-relaxation values vary with development between brain structures, and emphasize the need to correct for such age-related effects during any determination of potential changes from control values.

Keywords

Brain development; T2-relaxometry; Magnetic resonance imaging; Gray matter; White matter

[*]**Corresponding Author:** Ronald M. Harper, Ph.D., Department of Neurobiology, David Geffen School of Medicine at UCLA, University of California at Los Angeles, Los Angeles, CA 90095-1763, USA, rharper@ucla.edu, Tel: 310-825-5303, Fax: 310-825-2224.

INTRODUCTION

Several neurological, neuropsychological, and neuropsychiatric conditions are associated with brain changes in pediatric subjects [1–4], other than those accompanying normal aging [5]. Normal aging processes include rapid myelination and neuronal generation that reduce free tissue water content [6]. Neurodegenerative processes often show myelin and neuronal loss [7,8], which emerge with increased free water content. Disease-related tissue changes can be identified accurately only after partitioning age-related changes, and thus, normative description of developmental trends in different pediatric brain sites is required.

Magnetic resonance (MR) T2-relaxometry, the oldest MR procedure that has been used routinely in clinical evaluation [9,10], measures free tissue water content [11]. T2-relaxation values increase with increase in free water content [11], and free water content changes with disease and normal aging processes [5,12]. The procedure has been used to evaluate age-related brain myelin changes in pediatrics [13], and in several pediatric and adult medical conditions, demonstrating abnormalities not-readily-visible on conventional MRI, including traumatic brain injury [14], neurodegenerative conditions [4,7,15], cerebral neoplasia [16], ischemia [17], and symptomatic lesional epilepsy [18]. However, current T2-relaxometry data have primarily evaluated very young infants or adult subjects, and those studies principally examined only limited brain areas. The T2-relaxometry technique may be helpful in assessing developmental brain changes in gray and white matter of adolescent subjects.

The aim was to evaluate developmental changes in T2-relaxation values in regional brain sites, and sex differences in the T2-relaxation values for those sites in adolescents over the age range of 7 to 24 years.

MATERIALS AND METHODS

Subjects

Thirty one subjects (mean age ± SD: 17.4 ± 4.9 years; age range: 7–24 years; body-mass-index ± SD: 21.8 ± 4.7 kg/m^2; 18 male) participated. All subjects were without any diagnosed medical condition, such as neurological or other central nervous system-related disorders that could introduce brain tissue injury. All subjects were part of another brain imaging study, and were recruited through advertisements at the university campus and neighboring areas. We excluded subjects with conditions inappropriate for a high-magnetic field environment or that could introduce artifacts on brain images, as suggested by the web-site of the Institute for Magnetic Resonance Safety, Education, and Research (http://www.mrisafety.com/).

The University of California at Los Angeles Institutional Review Board approved the study, and all children and their parents/guardians provided informed written consent/assent prior to the study. We removed personal identifiable information of all subjects from the data evaluation records once analyses were completed.

Magnetic Resonance Imaging

Brain imaging studies were performed with a 3.0-Tesla MR imaging scanner (Magnetom Tim-Trio; Siemens, Erlangen, Germany), using a receive-only 8-channel phased-array head-coil, and a whole-body transmitter coil. We used foam pads on both sides of the head to reduce head motion. High-resolution T1-weighted images were acquired using a magnetization prepared rapid acquisition gradient-echo (MPRAGE) pulse sequence [repetition-time (TR) = 2200 ms; echo-time (TE) = 2.34 ms; inversion time = 900 ms; flip angle (FA) = 9°; matrix size = 320 × 320; field-of-view (FOV) = 230 × 230 mm; slice thickness = 0.9 mm; slices = 192]. Proton-density (PD) and T2-weighted images were

collected, covering the whole-brain, using a dual-echo turbo spin-echo pulse sequence (TR = 10,000 ms; TE1, 2 = 12, 119 ms; FA = 130°; matrix size = 256 × 256; FOV = 230 × 230 mm; slice thickness = 3.5 mm; turbo factor = 5). We used the generalized autocalibrating partially parallel acquisition (GRAPPA) parallel imaging technique with an acceleration factor of two for both scans.

Data Processing

We visually examined high-resolution T1-weighted, PD and T2-weighted images of all subjects for any major pathology, such as cystic lesions, tumors, or any other mass lesions to ensure that all brain images were acceptable to include for subsequent data processing. PD- and T2-weighted images were also evaluated for head motion-related or other imaging artifacts before T2-relaxation calculation.

We used the statistical parametric mapping package SPM8 (http://www.fil.ion.ucl.ac.uk/spm/), MRIcroN [19], and MATLAB-based (The MathWorks Inc., Natick, MA) custom software for data processing and analyses.

T2-relaxation calculation—We used PD and T2-weighted images for calculation of T2-relaxation values. The average noise level outside the brain parenchyma was calculated from PD and T2-weighted images, and was used as a masking threshold to exclude non-brain regions; we used the same masking threshold for the PD and T2-weighted images for all subjects. A ceiling threshold of 500 ms was applied to all T2-relaxtaion maps to limit cerebrospinal fluid (CSF) values. The following equation was used to calculate voxel-by-voxel T2-relaxation values using PD and T2-weighted images [18,20]:

$$T_2 = \frac{(TE_2 - TE_1)}{\ln\left(\frac{SI_1}{SI_2}\right)},$$

where TE_1 and TE_2 are the echo-times for PD and T2-weighted images, and SI_1, SI_2 represent PD and T2-weighted images signal intensities, respectively. We constructed whole-brain T2-relaxation maps using T2-relaxation values calculated for each voxel.

Normalization of T2-relaxation maps—T2-relaxation maps of all subjects were normalized to Montreal Neurological Institute (MNI) template space. We used T2-weighted images of each subject to determine normalization parameters, using *a priori*-defined distributions of different tissue types, including gray, white, and CSF [21], and the resulting normalization parameters were applied to corresponding T2-relaxation maps and T2-weighted images. The normalized T2-weighted images from all subjects were averaged to create mean background images.

Region of interest (ROI) analyses—Using mean background images, derived from normalized T2-weighted images, we created a set of rectangular regions of interest (ROIs) from different brain sites with MRIcroN. These brain areas were chosen from rostral (telencephalic), thalamic and hypothalamic (diencephalic), and pontine and cerebellar (metencephalic) regions (Fig. 1). We did not include medullary structures, since the proximity of CSF and minor misregistration of T2-relaxation maps to MNI common space might contaminate T2-relaxation values in those areas. Within each region, several sites were assessed using ROI. For smaller brain structures, the size of the ROI was chosen to fit within the structure, and all ROIs were extended to three slices of the brain for each structure.

Rostral brain: Regions of interest within the rostral brain were selected from the cortical gray and white matter, basal ganglia, hippocampus, and amygdala. Regions of interest were created for bilateral structures, including the anterior, mid, and posterior cingulate cortices, anterior, mid, and posterior insular cortices, caudate nuclei, putamen, globus pallidus, frontal white and gray matter, inferior, mid, and superior hippocampus, amygdala, inferior, mid, and superior temporal white matter, midline occipital gray matter, and occipital white matter. Unilaterally, structures included the anterior, mid, and posterior portions of the corpus callosum. The size of ROI samples varied from 27 to 243 mm^3, depending upon the brain structure.

Thalamus and hypothalamus: Regions of interest were selected from both thalamic and hypothalamic structures. We created ROI for both left and right structures, including the anterior, mid, and posterior thalamus, and hypothalamus. The size of ROIs varied from 12 to 75 mm^3 for these structures.

Pons and cerebellum: Regions of interest from the pons and cerebellum were outlined from the inferior, mid, and superior pons, cerebellar deep nuclei, and bilateral structures, including the caudal and rostral cerebellar cortices, and inferior, mid, and superior cerebellar peduncles. The size of the ROIs varied from structure to structure (27 to 147 mm^3).

Mean ROI T2-relaxation and R2 calculation: Using ROI brain masks created for different brain sites and normalized T2-relaxation maps, T2-relaxation values were extracted from those areas, and mean T2-relaxation values were calculated for each ROI. Using T2-relaxation values, R2 (1/T2) values of different brain regions were calculated and correlated with age to evaluate developmental trends.

Statistical Analyses

We used the Statistical Package for the Social Sciences (SPSS, V 18.0, Chicago, IL) software package for data analyses. Pearson's correlation procedures were used to assess the development of R2 values of different brain areas with age. Mean T2-relaxation value differences between males and females of those regions were also assessed with independent-samples t-tests. We considered a *p* value less than 0.05 statistically significant.

RESULTS

Rostral Brain

Brain regions within the rostral brain with positive correlations between R2 values and age are shown in scatter plots (Fig. 2, 3). These regions included the bilateral amygdalae (left, $r = 0.76$, $p < 0.001$; right, $r = 0.56$, $p = 0.001$), caudate nuclei (left, $r = 0.62$, $p < 0.001$; right, $r = 0.65$, $p < 0.001$), putamen (left, $r = 0.85$, $p < 0.001$; right, $r = 0.79$, $p < 0.001$), globus pallidus (left, $r = 0.70$, $p < 0.001$; right, $r = 0.71$, $p < 0.001$), mid hippocampus (left, $r = 0.56$, $p = 0.001$; right, $r = 0.37$, $p = 0.04$), inferior temporal white matter (left, $r = 0.60$, $p < 0.001$; right, $r = 0.46$, $p = 0.01$), anterior cingulate cortex (left, $r = 0.40$, $p = 0.028$; right, $r = 0.54$, $p = 0.002$), and left anterior ($r = 0.41$, $p = 0.021$) and posterior insula ($r = 0.43$, $p = 0.015$), mid cingulate ($r = 0.43$, $p = 0.015$), and inferior hippocampus ($r = 0.44$, $p = 0.013$). No regional negative correlations emerged between R2 values and age within the rostral brain.

Thalamus and Hypothalamus

Thalamic and hypothalamic brain sites with significant relationships between R2 values and age are shown in Fig. 4 scatter plots. Significant positive correlations appeared between R2 values of bilateral anterior (left, $r = 0.48$, $p = 0.007$; right, $r = 0.42$, $p = 0.018$), mid (left, r =

0.54, p = 0.002; right, r = 0.60, p < 0.001), and posterior thalamus (left, r = 0.39, p = 0.029; right, r = 0.53, p = 0.002) and age. No significant changes in R2 values appeared in the hypothalamus with age.

Pons and Cerebellum

Significant negative and positive correlations emerged between R2 values of brain regions within the cerebellum and age; these correlations are displayed on scatter plots (Fig. 5). Brain sites that showed negative correlations included the right mid (r = − 0.41, p = 0.021) and inferior cerebellar peduncles (r = − 0.43, p = 0.015), and a positive correlation emerged in the cerebellar deep nuclei (r = 0.37, p = 0.043).

Although all areas outlined in the scatter plots showed significant correlations between R2 values and age, multiple structures, often contralateral to, or in different subregions of structures showing correlations, showed no relationship of R2 values with age. These structures included the right anterior and posterior insula, mid cingulate, inferior hippocampus, left inferior and mid cerebellar peduncles, bilateral mid insula, superior hippocampus, frontal, occipital, and mid and superior temporal white matter, frontal and occipital gray matter, pons, corpus callosum, hypothalamus, and rostral and caudal cerebellar cortices.

Male Female Differences

No significant differences in age and body-mass-index appeared between male and female subjects (age, p = 0.13; body-mass-index, p = 0.59). Areas within the mid pons (p = 0.04), and left occipital white matter (p = 0.02) showed significant differences between males and females, with higher T2-relaxation values in males over females (Table 1, 3). No other brain sites showed significant T2-relaxation value differences between sexes (Tables 1–3).

DISCUSSION

Overview

R2 values largely increase (T2-relaxation values decline) with increasing age in adolescents in most brain sites, except for the cerebellar peduncles, where values decrease as the children mature. Significant male-female differences appear in T2-relaxation values in the mid pons and left occipital white matter, although no changes with age appear in those structures. The developmental trends in T2-relaxation values offer baseline values against which disease-related tissue changes can be assessed, and indicate the need for age- and sex-related correction of T2-relaxation values during such evaluation.

Positive Correlations Between R2 Values and Age

T2-relaxation values are highly sensitive to neuronal and myelin changes that are not obvious on visual evaluation, and are influenced by total amount and distribution of water and its interaction with the surrounding microstructural environment [22]. Increased T2-values appear in several medical conditions that increase tissue free water content, including vasogenic edema [11], demyelination [7], neuronal loss [8], infarction, and gliosis [18]. However, T2-values decline with development, as brain neurons and white matter mature [23]. Most regions within the brain showed positive correlations with R2 values (or inverse correlations with T2-relaxation values) and age. T2-relaxation values are higher at birth, and values decline rapidly with age in early infancy [23]. As the brain develops, neuronal structures become more densely packed [24], and myelination increases [25]; these conditions restrict free water content, and result in reduced T2-relaxation values or increased R2 values, a phenomenon that apparently continues through adolescence, as we show here. Iron deposition can also contribute to declining T2-relaxation values with age. Iron, which is

paramagnetic in nature, shortens T2-relaxation values [26]. However, iron deposition is less likely to contribute to the decline in T2-relaxation values with age here, since values declined over all of the brain (cortex, white matter, and deep brain areas), but iron is preferentially taken up in localized sites, such as the basal ganglia with age in adults [27]; it is unclear, however if similar deposition occurs in adolescence.

Negative Correlations Between R2 Values and Age

Regions within the cerebellar peduncles showed negative correlations of R2 values (or positive correlations of T2-relaxation values) with age. For most white matter structures, T2-relaxation values initially decline rapidly within the early pediatric period with brain maturation [23], and then show a slower increase with normal aging processes to certain brain areas in adulthood [28,29]. These findings of a negative correlation with R2 values and age found here suggest that myelination in these sites completes early, as opposed to other brain structures, consistent with traditional neuroanatomic studies [28,29].

Differences in T2-relaxation Values between Males and Females

The mid-pons and left occipital white matter showed higher T2-relaxation values in males over females. The pons is apparently more densely packed in females, relative to males, which results in reduced T2-relaxation values in females. Although no reports of T2-relaxation value differences in the pons between males and females exist, volumetric procedures in adults show that females have smaller pontine volumes over males [30], supporting the assumption of a more densely-packed structure. Since the mid-pons contains structures critical to breathing, pain, autonomic regulation, and motor function [31–35], sex-related differences in T2-relaxation values are of substantial importance for a number of disorders that appear in adolescence [36–38].

Left occipital white matter in males showed significantly increased T2-relaxation values over females. The total cerebral volume peaks earlier in females, compared to males [39] and certain brain regions, including occipital white matter, may mature earlier than other brain sites. Delayed white matter development within male occipital areas may result in the increased T2-relaxation values over females.

T2-relaxation Calculations with Two TEs

We used the two-point method for T2-relaxation calculations, which requires two TEs and assumes a single exponential decay [20]. Brain tissue, especially white matter, may have a multi-exponential decay [40], and many TEs are required to obtain more-accurate T2-relaxation values for precise evaluation of underlying microscopic tissue changes. However, procedures with multi-echo (e.g., 16 echos) do not cover the entire brain within a reasonable scan time, restricting use in clinical settings [41]. Dual-echo conventional spin-echo sequences provide reproducible T2-relaxation values that highly correlate to T2 values derived from multi-echo procedures [20]. Fluid attenuated inversion recovery (FLAIR)-based dual echo sequences may provide more appropriate findings than other sequences, including dual-echo conventional spin-echo (CSE) sequences [42], from suppression of cerebrospinal fluid (CSF), especially in areas where CSF is close to the tissue. However, in mesial temporal lobe pathology, both FLAIR and CSE procedures produce similar findings [43]. We used a fast spin-echo (FSE) sequence, which is routinely used in clinical practice, and acquires data rapidly with two TEs, including PD and T2-weighted images, and cover the entire brain [44]. T2-relaxation values derived for FSE-based sequences are highly stable and reproducible, and show high correlations with T2-values obtained from multi-echo methods [44]. Also, we used a ceiling threshold to limit CSF values during T2-relaxation calculations to reduce contamination from CSF values. Although FSE-based sequences may

not provide precise T2-relaxation values, the procedure has several advantages over the others in diagnostic and research-related imaging.

Conclusions

Significant positive or negative correlations appeared between age and R2 values of multiple brain sites, indicating that water content can vary substantially between brain regions during adolescence. No significant differences emerged in T2-relaxation values between males and females for most brain sites, except for the mid-pons and left occipital white matter, in which males showed higher values over females. The present description of developmental trends in T2-relaxation values in different brain sites provides a baseline against which disease processes can be evaluated. The findings also emphasize the necessity for correction of T2-relaxation values for age and sex during any assessment of potential changes from normal values.

Acknowledgments

Authors thank Ms. Rebecca Harper and Mr. Edwin M. Valladares for assistance with data collection, and Dr. Jennifer Ogren for scientific editing. This research was supported by the National Institute of Child Health and Human Development R01 HD-22695.

REFERENCES

1. Johnson MA, Pennock JM, Bydder GM, Steiner RE, Thomas DJ, Hayward R, Bryant DR, Payne JA, Levene MI, Whitelaw A, Dubowitz LMS, Dubowitz V. Clinical NMR imaging of the brain in children: normal and neurologic disease. Am J Roentgenol 1983;141(5):1005–1018. [PubMed: 6605040]
2. Zafeiriou DI, Anastasiou AL, Michelakaki EM, Augoustidou-Savvopoulou PA, Katzos GS, Kontopoulos EE. Early infantile Krabbe disease: deceptively normal magnetic resonance imaging and serial neurophysiological studies. Brain Dev 1997;19(7):488–491. [PubMed: 9408597]
3. Boes AD, McCormick LM, Coryell WH, Nopoulos P. Rostral anterior cingulate cortex volume correlates with depressed mood in normal healthy children. Biol Psychiatry 2008;63(4):391–397. [PubMed: 17916329]
4. Williamson P, Pelz D, Merskey H, Morrison S, Karlik S, Drost D, Carr T, Conlon P. Frontal, temporal, and striatal proton relaxation times in schizophrenic patients and normal comparison subjects. Am J Psychiatry 1992;149(4):549–551. [PubMed: 1554045]
5. Yakovlev, PILA. The myelogenetic cycles of regional maturation of the brain. In: Minkrowski, A., editor. Regional development of the brain in early life. Oxford: Blackwell; 1967. p. 3-70.
6. Dobbing J, Sands J. Quantitative growth and development of human brain. Arch Dis Child 1973;48(10):757–767. [PubMed: 4796010]
7. Seewann A, Vrenken H, van der Valk P, Blezer EL, Knol DL, Castelijns JA, Polman CH, Pouwels PJ, Barkhof F, Geurts JJ. Diffusely abnormal white matter in chronic multiple sclerosis: imaging and histopathologic analysis. Arch Neurol 2009;66(5):601–609. [PubMed: 19433660]
8. Wegner C, Esiri MM, Chance SA, Palace J, Matthews PM. Neocortical neuronal, synaptic, and glial loss in multiple sclerosis. Neurology 2006;67(6):960–967. [PubMed: 17000961]
9. Bernasconi A, Bernasconi N, Caramanos Z, Reutens DC, Andermann F, Dubeau F, Tampieri D, Pike BG, Arnold DL. T2 relaxometry can lateralize mesial temporal lobe epilepsy in patients with normal MRI. NeuroImage 2000;12(6):739–746. [PubMed: 11112405]
10. Damadian R. Tumor detection by nuclear magnetic resonance. Science 1971;171(976):1151–1153. [PubMed: 5544870]
11. Loubinoux I, Volk A, Borredon J, Guirimand S, Tiffon B, Seylaz J, Meric P. Spreading of vasogenic edema and cytotoxic edema assessed by quantitative diffusion and T2 magnetic resonance imaging. Stroke 1997;28(2):419–426. [PubMed: 9040700]

12. Larsson HB, Frederiksen J, Kjaer L, Henriksen O, Olesen J. In vivo determination of T1 and T2 in the brain of patients with severe but stable multiple sclerosis. Magn Reson Med 1988;7(1):43–55. [PubMed: 3386521]
13. Ono J, Kodaka R, Imai K, Itagaki Y, Tanaka J, Inui K, Nagai T, Sakurai K, Harada K, Okada S. Evaluation of myelination by means of the T2 value on magnetic resonance imaging. Brain Dev 1993;15(6):433–438. [PubMed: 8147502]
14. Mamere AE, Saraiva LA, Matos AL, Carneiro AA, Santos AC. Evaluation of delayed neuronal and axonal damage secondary to moderate and severe traumatic brain injury using quantitative MR imaging techniques. Am J Neuroradiol 2009;30(5):947–952. [PubMed: 19193759]
15. Laakso MP, Partanen K, Soininen H, Lehtovirta M, Hallikainen M, Hanninen T, Helkala EL, Vainio P, Riekkinen PJ Sr. MR T2 relaxometry in Alzheimer's disease and age-associated memory impairment. Neurobiol Aging 1996;17(4):535–540. [PubMed: 8832627]
16. Kurki T, Komu M. Spin-lattice relaxation and magnetization transfer in intracranial tumors in vivo: effects of Gd-DTPA on relaxation parameters. Magn Reson Imaging 1995;13(3):379–385. [PubMed: 7791547]
17. Jacobs MA, Mitsias P, Soltanian-Zadeh H, Santhakumar S, Ghanei A, Hammond R, Peck DJ, Chopp M, Patel S. Multiparametric MRI tissue characterization in clinical stroke with correlation to clinical outcome: part 2. Stroke 2001;32(4):950–957. [PubMed: 11283396]
18. Kumar R, Gupta RK, Rathore RK, Rao SB, Chawla S, Pradhan S. Multiparametric quantitation of the perilesional region in patients with healed or healing solitary cysticercus granuloma. NeuroImage 2002;15(4):1015–1020. [PubMed: 11906241]
19. Rorden C, Karnath HO, Bonilha L. Improving lesion-symptom mapping. J Cogn Neurosci 2007;19(7):1081–1088. [PubMed: 17583985]
20. Duncan JS, Bartlett P, Barker GJ. Technique for measuring hippocampal T2 relaxation time. Am J Neuroradiol 1996;17(10):1805–1810. [PubMed: 8933861]
21. Ashburner J, Friston KJ. Unified segmentation. NeuroImage 2005;26(3):839–851. [PubMed: 15955494]
22. Mathur-De Vre R. Biomedical implications of the relaxation behaviour of water related to NMR imaging. Br J Radiol 1984;57(683):955–976. [PubMed: 6100168]
23. Masumura M. Proton relaxation time of immature brain. II. In vivo measurement of proton relaxation time (T1 and T2) in pediatric brain by MRI. Childs Nerv Syst 1987;3(1):6–11. [PubMed: 3594473]
24. Reiss AL, Abrams MT, Singer HS, Ross JL, Denckla MB. Brain development, gender and IQ in children. A volumetric imaging study. Brain 1996;119(Pt 5):1763–1774. [PubMed: 8931596]
25. Barkovich AJ. Concepts of myelin and myelination in neuroradiology. Am J Neuroradiol 2000;21(6):1099–1109. [PubMed: 10871022]
26. Vymazal J, Brooks RA, Baumgarner C, Tran V, Katz D, Bulte JW, Bauminger R, Di Chiro G. The relation between brain iron and NMR relaxation times: an in vitro study. Magn Reson Med 1996;35(1):56–61. [PubMed: 8771022]
27. Aquino D, Bizzi A, Grisoli M, Garavaglia B, Bruzzone MG, Nardocci N, Savoiardo M, Chiapparini L. Age-related iron deposition in the basal ganglia: quantitative analysis in healthy subjects. Radiology 2009;252(1):165–172. [PubMed: 19561255]
28. Hasan KM, Halphen C, Boska MD, Narayana PA. Diffusion tensor metrics, T2 relaxation, and volumetry of the naturally aging human caudate nuclei in healthy young and middle-aged adults: possible implications for the neurobiology of human brain aging and disease. Magn Reson Med 2008;59(1):7–13. [PubMed: 18050345]
29. Agartz I, Saaf J, Wahlund LO, Wetterberg L. T1 and T2 relaxation time estimates in the normal human brain. Radiology 1991;181(2):537–543. [PubMed: 1924801]
30. Raz N, Gunning-Dixon F, Head D, Williamson A, Acker JD. Age and sex differences in the cerebellum and the ventral pons: a prospective MR study of healthy adults. Am J Neuroradiol 2001;22(6):1161–1167. [PubMed: 11415913]
31. McGinty DJ, Harper RM. Dorsal raphe neurons: depression of firing during sleep in cats. Brain Res 1976;101(3):569–575. [PubMed: 1244990]

32. Fenik VB, Davies RO, Kubin L. REM sleep-like atonia of hypoglossal (XII) motoneurons is caused by loss of noradrenergic and serotonergic inputs. Am J Respir Crit Care Med 2005;172(10):1322–1330. [PubMed: 16100007]
33. Goadsby PJ, Piper RD, Lambert GA, Lance JW. Effect of stimulation of nucleus raphe dorsalis on carotid blood flow. II. The cat. Am J Physiol 1985;248(2 Pt 2):R263–R269. [PubMed: 2857529]
34. Ni HF, Zhang JX, Harper RM. Respiratory-related discharge of periaqueductal gray neurons during sleep-waking states. Brain Res 1990;511(2):319–325. [PubMed: 2334849]
35. Keay KA, Crowfoot LJ, Floyd NS, Henderson LA, Christie MJ, Bandler R. Cardiovascular effects of microinjections of opioid agonists into the 'Depressor Region' of the ventrolateral periaqueductal gray region. Brain Res 1997;762(1–2):61–71. [PubMed: 9262159]
36. Kumar R, Macey PM, Woo MA, Alger JR, Keens TG, Harper RM. Neuroanatomic deficits in congenital central hypoventilation syndrome. J Comp Neurol 2005;487(4):361–371. [PubMed: 15906312]
37. Halbower AC, Degaonkar M, Barker PB, Earley CJ, Marcus CL, Smith PL, Prahme MC, Mahone EM. Childhood obstructive sleep apnea associates with neuropsychological deficits and neuronal brain injury. PLoS Med 2006;3(8):e301. [PubMed: 16933960]
38. Huguet A, Miro J. The severity of chronic pediatric pain: an epidemiological study. J Pain 2008;9(3):226–236. [PubMed: 18088558]
39. Lenroot RK, Gogtay N, Greenstein DK, Wells EM, Wallace GL, Clasen LS, Blumenthal JD, Lerch J, Zijdenbos AP, Evans AC, Thompson PM, Giedd JN. Sexual dimorphism of brain developmental trajectories during childhood and adolescence. NeuroImage 2007;36(4):1065–1073. [PubMed: 17513132]
40. Dula AN, Gochberg DF, Valentine HL, Valentine WM, Does MD. Multiexponential T2, magnetization transfer, and quantitative histology in white matter tracts of rat spinal cord. Magn Reson Med 63(4):902–909. [PubMed: 20373391]
41. Jackson GD, Connelly A, Duncan JS, Grunewald RA, Gadian DG. Detection of hippocampal pathology in intractable partial epilepsy: increased sensitivity with quantitative magnetic resonance T2 relaxometry. Neurology 1993;43(9):1793–1799. [PubMed: 8414034]
42. Melhem ER, Whitehead RE, Bert RJ, Caruthers SD. MR imaging of the hippocampus: measurement of T2 with four dual-echo techniques. Radiology 1998;209(2):551–555. [PubMed: 9807588]
43. Woermann FG, Steiner H, Barker GJ, Bartlett PA, Elger CE, Duncan JS, Symms MR. A fast FLAIR dual-echo technique for hippocampal T2 relaxometry: first experiences in patients with temporal lobe epilepsy. J Magn Reson Imaging 2001;13(4):547–552. [PubMed: 11276098]
44. Okujava M, Schulz R, Ebner A, Woermann FG. Measurement of temporal lobe T2 relaxation times using a routine diagnostic MR imaging protocol in epilepsy. Epilepsy Res 2002;48(1–2):131–142. [PubMed: 11823117]

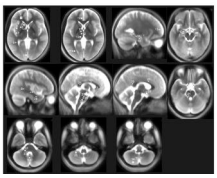

Figure 1.

Brain regions showing regions of interest (ROIs) on mean background images, with ROIs represented by rectangles proportional to volumes collected and used for T2-relaxation calculations. ROIs are overlaid onto mean background images, derived from normalized T2-weighted images; for clarity, only left-sided ROIs are displayed. 1, frontal white matter; 2, caudate nucleus; 3, putamen; 4, globus pallidus; 5, anterior insula; 6, mid insula; 7, posterior insula; 8, superior temporal white matter; 9, midline occipital gray matter; 10, anterior cingulate; 11, anterior thalamus; 12, mid thalamus; 13, posterior thalamus; 14, occipital white matter; 15, frontal cortex; 16, inferior hippocampus; 17, mid hippocampus; 18, superior hippocampus; 19, amygdala; 20, inferior temporal white matter; 21, mid temporal white matter; 22, anterior corpus callosum; 23, mid corpus callosum; 24, posterior corpus callosum; 25, superior pons; 26, mid pons; 27, inferior pons; 28, mid cingulate; 29, posterior cingulate; 30, hypothalamus; 31, superior cerebellar peduncle; 32, mid cerebellar peduncle; 33, inferior cerebellar peduncle; 34 cerebellar deep nuclei; 35, rostral cerebellar cortex; 36, caudal cerebellar cortex.

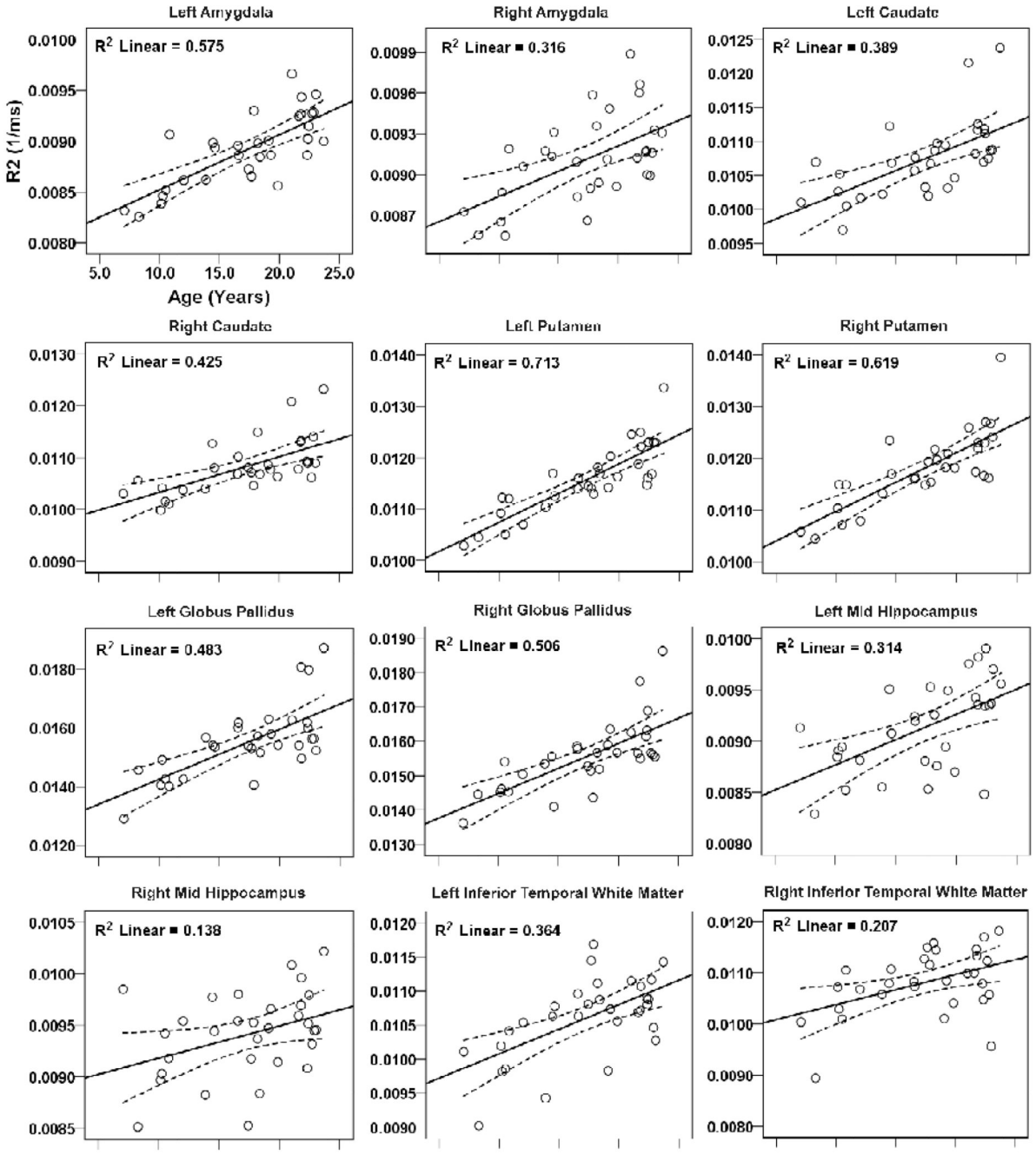

Figure 2.

Brain regions within the rostral brain (telencephalon), including the amygdala, caudate, putamen, globus pallidus, hippocampus, and temporal white matter showing significant correlations between R2 values and age. Solid lines show best fit lines for the data, and dotted lines above and below the best fit line show 95% mean confidence intervals.

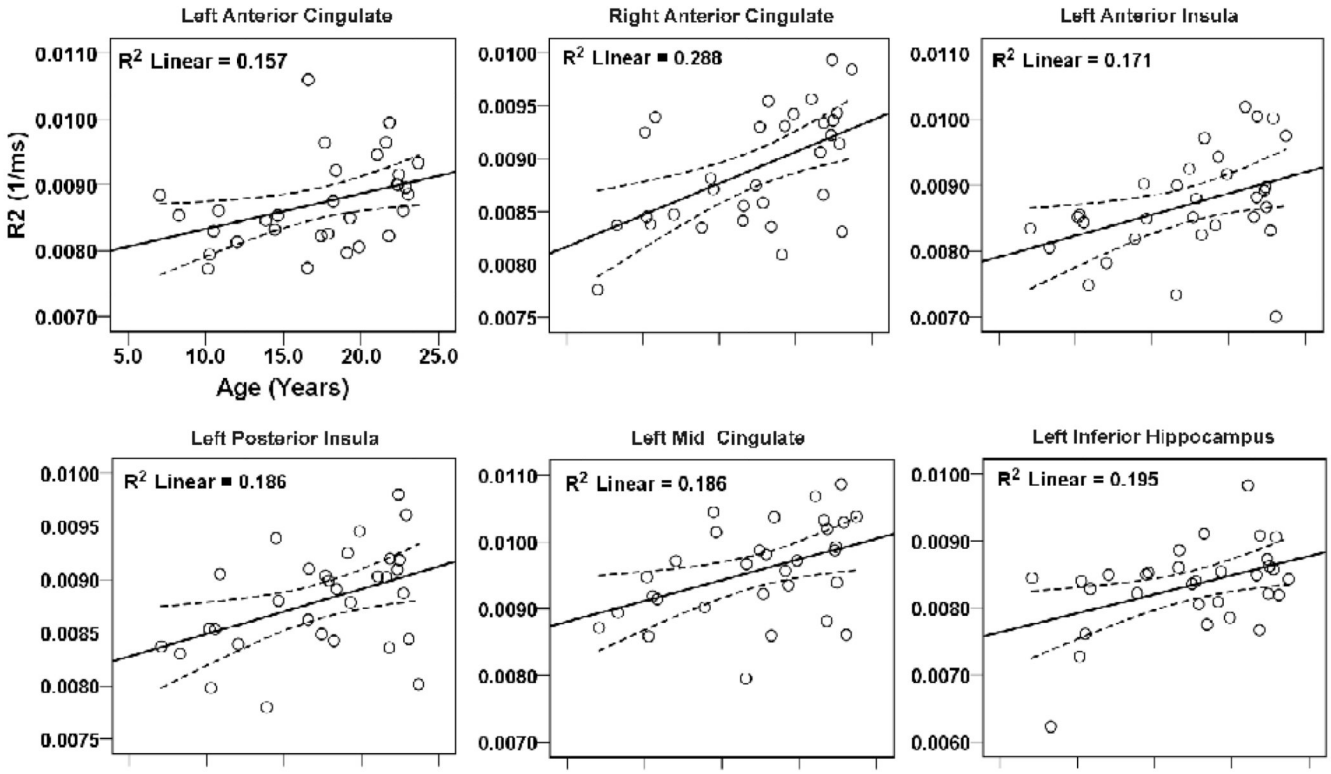

Figure 3.

Brain areas within the cingulate, insula, and hippocampus showing significant correlations between R2 values and age. Figure conventions are the same as in Figure 2.

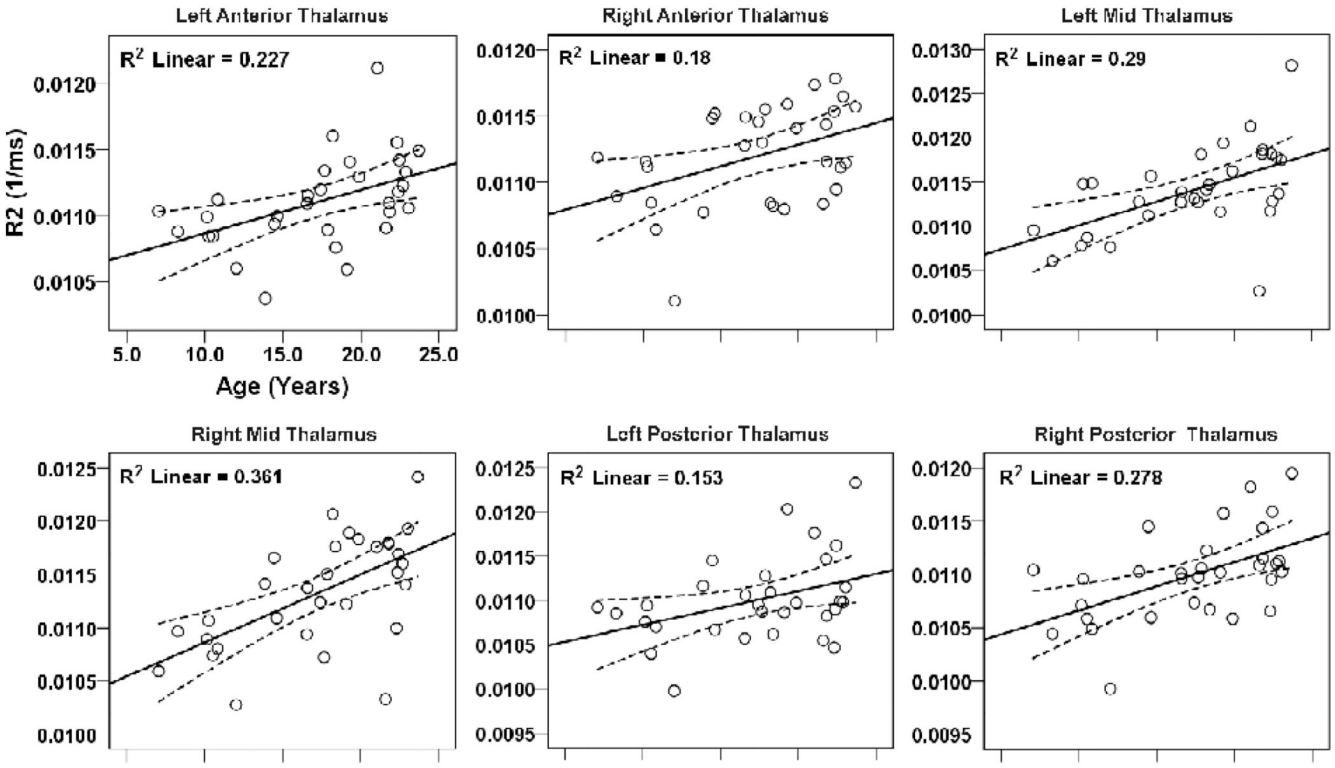

Figure 4.
Brain sites within the thalamus showing significant correlations between regional R2 values and age. Figure conventions are the same as in Figure 2.

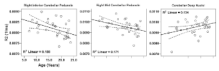

Figure 5.
Multiple brain areas in the cerebellar peduncles and deep nuclei that show significant correlations between R2 values and age. Figure conventions are the same as in Figure 2.

Table 1

T2-relaxation values of brain sites within the rostral brain (telencephalon), including cortical, basal ganglia, amygdala, and hippocampal structures, and male-female differences.

Brain Structures (ROI size, 27–243 mm^3)	T2 values (ms) (n = 31)	T2 values (ms) (male, n = 18)	T2 values (ms) (female, n = 13)
L Amygdala	112.3±4.4	111.2±4.4	113.7±4.2
R Amygdala	109.9±3.9	109.2±3.7	110.8±4.1
L Anterior Cingulate	115.2±8.5	114.2±9.4	116.5±7.1
R Anterior Cingulate	112.7±7.0	112.0±6.7	113.6±7.6
L Mid Cingulate	105.0±8.0	103.4±9.0	107.3±6.1
R Mid Cingulate	103.8±9.0	103.4±10.3	104.2±7.4
L Posterior Cingulate	105.5±14.5	103.8±12.2	108.0±17.4
R Posterior Cingulate	106.7±18.9	104.2±11.1	110.3±26.3
Anterior Corpus Callosum	81.0±4.4	81.2±4.3	80.9±4.7
Mid Corpus Callosum	109.4±15.1	109.6±14.8	109.2±16.1
Posterior Corpus Callosum	87.5±6.8	86.8±7.5	88.5±5.8
L Anterior Insula	115.7±10.4	115.1±12.1	116.7±8.0
R Anterior Insula	111.9±20.3	116.0±25.4	106.2±7.7
L Mid Insula	123.0±10.4	123.6±10.1	122.2±11.3
R Mid Insula	111.0±8.6	110.4±7.8	111.8±9.9
L Posterior Insula	114.0±6.3	113.4±7.5	114.7±4.4
R Posterior Insula	108.1±6.2	108.8±7.0	107.1±5.1
L Caudate Nuclei	93.3±4.7	92.5±5.3	94.5±3.6
R Caudate Nuclei	92.5±4.3	91.8±4.6	93.5±3.7
L Frontal Gray Matter	131.6±16.4	128.5±15.9	135.9±16.8
R Frontal Gray Matter	120.1±13.6	119.8±14.9	120.4±12.2
L Frontal White Matter	88.5±4.1	88.8±4.0	88.1±4.5
R Frontal White Matter	85.3±3.8	85.9±3.0	84.6±4.8
L Globus Pallidus	64.8±4.9	64.5±4.0	65.3±6.1
R Globus Pallidus	64.5±4.0	63.8±3.3	65.6±4.8
L Putamen	86.6±5.0	85.8±4.9	87.7±5.1
R Putamen	85.0±5.1	84.2±5.1	86.0±5.0
L Inf Hippocampus	120.7±10.2	117.9±6.8	124.6±13.0
R Inf Hippocampus	116.7±6.1	115.2±6.1	118.9±5.8
L Mid Hippocampus	109.7±5.3	108.5±4.9	111.4±5.4
R Mid Hippocampus	106.5±4.8	105.3±4.0	108.2±5.4
L Sup Hippocampus	114.3±5.4	114.3±6.8	114.3±3.0
R Sup Hippocampus	114.9±14.6	113.1±10.7	117.4±19.0
L Inf Temp White Matter	94.5±5.5	94.0±5.2	95.3±6.1
R Inf Temp White Matter	92.9±5.8	93.3±4.4	92.2±7.4

Brain Structures (ROI size, 27–243 mm^3)	**T2 values (ms) (n = 31)**	**T2 values (ms) (male, n = 18)**	**T2 values (ms) (female, n = 13)**
L Mid Temp White Matter	91.3±3.9	90.8±4.6	91.9±2.6
R Mid Temp White Matter	88.8±3.7	88.5±3.0	89.2±4.5
L Sup Temp White Matter	96.2±3.1	96.4±3.2	96.0±3.1
R Sup Temp White Matter	92.3±2.9	92.6±3.2	91.8±2.6
L Midl Occi Gray Matter	111.0±12.1	109.7±10.3	112.8±14.4
R Midl Occi Gray matter	105.4±9.1	105.8±10.3	105.0±7.3
L Occi White Matter*	99.5±3.4	100.6±3.6	97.9±2.4
R Occi White Matter	96.1±3.3	96.8±3.7	95.2±2.6

ROI = Region of interest; L = Left; R = Right; Inf = Inferior; Sup = Superior; Temp = Temporal; Midl = Midline; Occi = Occipital;

* = $p < 0.05$ between males and females.

Table 2

T2-relaxation values of selected brain sites within the thalamus and hypothalamus, and male female differences.

Brain Structures (ROI size, 12–75 mm^3)	T2 values (ms) (n = 31)	T2 values (ms) (male, n = 18)	T2 values (ms) (female, n = 13)
L Anterior Thalamus	90.1±2.7	90.1±3.1	90.0±2.3
R Anterior Thalamus	89.4±3.1	89.0±3.5	90.0±2.6
L Mid Thalamus	87.8±3.8	87.3±4.3	88.5±3.0
R Mid Thalamus	88.4±4.1	88.2±4.4	88.7±3.9
L Posterior Thalamus	91.0±3.9	91.2±4.3	90.7±3.3
R Posterior Thalamus	91.0±3.5	90.8±3.8	91.3±3.3
L Hypothalamus	107.0±5.0	106.5±5.6	107.6±4.3
R Hypothalamus	111.2±15.0	111.0±14.3	111.4±16.5

ROI = Region of interest; L = Left; R = Right.

Table 3

T2-relaxation values of selected brain sites within the cerebellum and pons, and male-female differences.

Brain Structures (ROI size, 27–147 mm^3)	T2 values (ms) (n = 31)	T2 values (ms) (male, n = 18)	T2 values (ms) (female, n = 13)
Sup Pons	91.0±10.6	92.3±10.9	89.2±10.4
Mid Pons*	93.9±8.4	96.5±8.1	90.4±7.7
Inf Pons	97.1±8.1	98.1±8.9	95.7±6.9
L Cau Cereb Cortex	114.9±5.4	116.0±4.8	113.5±6.0
R Cau Cereb Cortex	111.0±5.0	111.0±4.5	110.8±5.7
L Ros Cereb Cortex	110.9±4.7	110.2±4.5	111.8±5.0
R Ros Cereb Cortex	103.7±5.7	103.9±3.4	103.4±8.1
Cereb Deep Nuclei	106.0±8.7	104.6±5.2	107.9±12.1
L Inf Cereb Peduncle	121.8±6.2	121.9±6.2	121.6±6.4
R Inf Cereb Peduncle	122.8±6.0	122.1±6.1	123.7±5.9
L Mid Cereb Peduncle	105.4±6.5	106.4±6.6	104.0±6.3
R Mid Cereb Peduncle	105.3±7.1	107.2±8.2	102.6±4.2
L Sup Cereb Peduncle	110.1±6.7	110.7±5.2	109.4±8.6
R Sup Cereb Peduncle	108.2±6.2	108.6±6.0	107.5±6.6

ROI = Region of interest; Sup = Superior; Inf = Inferior; L = Left; Cau = Caudal; Cereb = Cerebellar; R = Right; Ros = Rostral;

* = $p < 0.05$ between males and females.